INTERSPEECH 2021
30 August – 3 September, 2021, Brno, Czechia

Group Delay based Re-weighted Sparse Recovery Algorithms for Robust and High-Resolution Source Separation in DOA Framework

Murtiza Ali , Ashwani Koul, Karan Nathwani

IIT Jammu, India

2020ree2059@iitjammu.ac.in, ashvinikoul1993@gmail.com, karan.nathwani@iitjammu.ac.in

Abstract

Sparse Recovery (SR) algorithms have been used widely for direction-of-arrival (DOA) estimation in spatially contiguous plane wave for their robust performance. But these algorithms have proven to be computationally costly. With a few sensors and at low SNRs, the noise dominates the data singular vectors and the sparse estimation of contiguous sources is incorrect. The magnitude spectrum-based re-weighted sparse recovery (RWSR) algorithms improve the robustness by re-weighting the sparse estimates. However, their efficiency degrades with decreasing the number of sensors at low SNRs. Therefore, this paper exhibits the significance of the phase spectrum, in the form of group-delay, for sparse and robust source estimation using RWSR algorithms for spatially contiguous sources. Further, an optimal re-weighted methodology based on simultaneously minimizing average-root-mean-square-error and maximizing the probability of separation is also proposed. The simulation results are carried out for Gaussian noise to demonstrate the excellent performance of the proposed algorithms.

Index Terms: Source Separation, DOA Estimation, Group-delay, low SNR, Phase Spectrum, RWSR

1. Introduction

Direction-of-arrival (DOA) and source localization estimation of incoming signals has been an active area of research in SONAR & RADAR for decades [1] [2]. Several beamforming techniques such as delay-sum-beamformer (DSB) [3], adaptive beamforming methods like Capon beamformer [4] and subspace methods such as MUSIC, DeepMUSIC [5], min-norm, and ESPRIT [1] have been used extensively.

Recently, a robust and high-resolution DOA estimation based on the Sparse Recovery (SR) algorithms (following the convex optimization (CS) framework) [6, 7, 8] have gained popularity. It offers to exhibit high resolution source separability even at a low SNRs with a fewer snapshots even in the presence of noise. Many SR algorithms have been developed such as traditional ℓ_1 minimization [7, 9], ℓ_1-SVD and variants [8, 10, 11, 12], Sparse Recovery Weighted Subspace Fitting (SRWSF) [6], which search over a discrete grid. The computation complexity of these algorithms increases cubically with the number of search grid points [13]. The computation time also increases super-linearly with the increase in the number of snapshots for ℓ_1 minimization, whereas it remains fixed for ℓ_1-SVD SR algorithms [8, 14]. Some studies perform the search over a continuous grid such as Atomic or TV-norm based ℓ_1 minimization [15]. For contiguous sources at low SNRs, the SR-algorithms tend to face challenges in source separability, as noise dominates the top singular vectors of the data [8, 6]. However, the sparse DOA estimates of the signal vector are not robust due to increase in the steering matrix's condition number. To resolve this issue, the re-weighting of the sparse estimates is proposed [16, 17]. The re-weighted SR algorithms (RWSR) promotes sparsity and noise robustness by weighing the estimated sparse signal vector elements differently [16, 17, 18, 19]. For ℓ_1-SVD, the weights are calculated based on the orthogonality between the signal and noise vectors [17]. However, with a fewer sensors and at low SNR values (limiting the measurements), the performance of RWSR algorithms is degraded significantly [2, 7]. For narrowband sources, the high resolution and robustness property of group delay spectrum has been widely used in the context of formant estimation [20], in source separation [21, 22, 23, 24] and epoch extraction [25]. Computation of group-delay results in sharp peaks at the true DOAs with less sensitivity to the number of sensors. However, the group-delay estimator is sensitive to noise, reverberations and the array perturbations [26] which can be mitigated by multiplying group-delay with the MUSIC magnitude spectrum to remove the same. The eigenvalues are then estimated by shrinkage estimation techniques, as described in [27]. Although the MUSIC-Group Delay estimator improves the resolution (source separability) performance, it is sensitive to noise. The noise robustness property of the Group Delay function has not been significant in the context of DOA estimation at very low SNRs [27, 26, 28, 29].

Combining the group-delay function's high-resolution source separability property with the SR algorithms leads to an improved performance of DOA estimation of spatially contiguous signals with a fewer sensors at low SNRs, which suits real-time applications. Additionally the computational burden is reduced with few sensors, fixed data singular vectors, and grid-refinement techniques. Further, an optimal re-weighted methodology based on simultaneously minimizing average-root-mean-square-error and maximizing the probability of separation is also proposed. The rest of paper is organized as follows: The array data model and the ℓ_1 minimization technique in the form of ℓ_1-SVD is presented in Section 2. Proposed re-weighted methodologies are discussed in Section 3. The simulation results are carried out in Section 4 which is followed by a brief conclusion in Section 5.

2. Problem Statement

Consider a uniform linear array (ULA) of *N* sensor elements :

$$\mathbf{Y} = \mathbf{AS} + \mathbf{N} \quad \in \mathbb{C}^{N \times L} \tag{1}$$

where $\mathbf{S}$ is a vector of amplitudes of incoming signals, $\mathbf{A}$ being the array steering vector and $\mathbf{N}$ the noise model vector, which is an independent and identical (i.i.d) circularly symmetric com-

Copyright © 2021 ISCA

http://dx.doi.org/10.21437/Interspeech.2021-164

plex Gaussian noise vector with zero mean and diagonal covariance matrix, i.e, $\mathbf{n}(t) \sim C\mathcal{N}(\mathbf{0}, \sigma^2\mathbf{I})$ [30]. Here, number of snapshots L are observed for the estimation process. The array manifold matrix is written as $\mathbf{A} = [\mathbf{a}(\theta_1), \mathbf{a}(\theta_2), \ldots, \mathbf{a}(\theta_J)] \in \mathbb{C}^{N\times J}$ where *J* is the narrow band source signal. The signal amplitude and array noise matrix are represented by $\mathbf{S} \in \mathbb{C}^{J\times L}$ and $\mathbf{N} \in \mathbb{C}^{N\times L}$ respectively. The measurement model can be recasted as sparse vector estimation process by defining an over-complete basis $\mathbf{A}_\Omega \in \mathcal{C}^{N\times K}$ of steering vectors formed by taking discrete set of spatial angles. With the knowledge of over-complete basis $\mathbf{A}_\Omega$ ($J \ll K$), Eq. 1 can be re-written as:

$$\mathbf{Y} = \mathbf{A}_\Omega\hat{\mathbf{S}} + \mathbf{N}, \tag{2}$$

where $\hat{\mathbf{S}} \in \mathbb{C}^{K\times L}$.

2.1. ℓ_1-SVD

The ℓ_1-SVD method is computationally efficient in terms of snapshots [8]. The grid refinement technique is one of the methods to reduce the search grid dimension. The number of measurements should be of order, $N \sim O(J\log(K/J))$ [31, 32, 13]. For ℓ_1-SVD method, considering the SVD of the data matrix given in Eq. (2)

$$\mathbf{Y} = \mathbf{U}\mathbf{\Lambda}\mathbf{V}^H. \tag{3}$$

We define

$$\tilde{\mathbf{Y}} = \mathbf{U}\mathbf{\Lambda}\mathbf{E}_J = \mathbf{Y}\mathbf{V}\mathbf{E}_J \in \mathbb{C}^{(N\times J)}, \tag{4}$$

where $\mathbf{E}_J = [\mathbf{I}_J \ \mathbf{0}]^T \in \mathbb{C}^{(L\times J)}$, $\mathbf{I}_J$ is the $(J \times J)$ identity matrix, and $\mathbf{0}$ being $J \times (L - J)$ zero-matrix. The Eq. (4) can be re-written as

$$\tilde{\mathbf{Y}} = \mathbf{A}_\Omega\tilde{\mathbf{S}} + \tilde{\mathbf{N}}, \tag{5}$$

where $\tilde{\mathbf{S}} = \hat{\mathbf{S}}\mathbf{V}\mathbf{E}_J$ and $\tilde{\mathbf{N}} = \mathbf{N}\mathbf{V}\mathbf{E}_J$. Most of the signal power is retained by the data matrix $\tilde{\mathbf{Y}}$. The row-support of $\tilde{\mathbf{S}}$ is identical to that of $\hat{\mathbf{S}}$. The columns of $\tilde{\mathbf{Y}}$ can be expressed as

$$\tilde{\mathbf{y}}(j) = \mathbf{A}_\Omega\tilde{\mathbf{s}}(j) + \tilde{\mathbf{n}}(j), j = 1, \ldots, J. \tag{6}$$

Let us define $s_k^{(\ell_2)} = \sqrt{\sum_{j=1}^{J}|\tilde{s}_k(j)|^2}, k = 1, \ldots, K$, where $\tilde{s}_k(j)$ denotes the k^{th} element of $\tilde{\mathbf{s}}(j)$. Collectively, a row vector is formed by $s_k^{(\ell_2)}$ which is given below:

$$\bar{\mathbf{s}}^{(\ell_2)} = [s_1^{(\ell_2)}, \ldots, s_K^{(\ell_2)}]^T \in \mathbb{R}^K. \tag{7}$$

It is observed that the support of $\bar{\mathbf{s}}^{(\ell_2)}$ is similar to the row-support of $\tilde{\mathbf{S}}$ and hence, it is worth considering $\bar{\mathbf{s}}$ a good approximation to the spatial magnitude spectrum. Thus, the $\bar{\mathbf{s}}^{(\ell_2)}$ can be recovered by solving the optimization problem [8]

$$\min ||\bar{\mathbf{s}}^{(\ell_2)}||_1 \text{ subject to } ||\tilde{\mathbf{Y}} - \mathbf{A}_\Omega\tilde{\mathbf{S}}||_F^2 \le \eta^2, \tag{8}$$

where $||\cdot||_F$ denotes the Frobenius norm and η is a regularization parameter that specifies how much noise is to be allowed. The value of η depends upon the noise and should be large enough such that probability $||\tilde{\mathbf{N}}||_F^2 \ge \eta^2$ is small.

2.1.1. Gaussian Noise in ℓ_1-SVD minimization

If the noise elements $\{\mathbf{n}(1), \ldots, \mathbf{n}(L)\}$ are i.i.d. complex circular Gaussian random variables with variance σ^2. It is shown in [8, 33] that $||(\sqrt{2}/\sigma)\tilde{\mathbf{N}}||_F^2$ has approximately a χ^2 distribution with a degrees of freedom $2NJ$ for moderate to high values of SNR. With the knowledge of the distribution, the confidence interval for $||\tilde{\mathbf{N}}||_F^2$ can be found. It is worth noting that its uppermost value can be considered as a choice for η^2.

2.2. Impact of ℓ_1-SVD with Number of Sensors and Closely Spaced Sources

Two major reasons for ℓ_1-SVD degradation are (a) the increase in the condition number of the steering matrix, which increases when the sources are contiguous, (b) the domination of noise on top data singular vectors at low SNRs [8]. To enhance the performance, the re-weighted methodology based on the orthogonality of signal and noise subspace have also been used in [17]. Although, such re-weighted methodologies enhance both sparsity and robustness of the SR processors. When the sources are contiguous, the RW-SR algorithms fail to resolve the sources correctly. The weight vector (computed using the magnitude spectrum) fails to consider two weights at low-SNR and with a few sensors. Hence, we propose a re-weighting methodology which not only enhances the sparsity and robustness but also the resolution performance of the SR algorithms with a fewer number of sensors and low values of SNR.

3. Proposed Re-weighted Methods for Source Separability in DOA estimation

We utilize high-resolution source separability property of Group-Delay Function (GDF) to enhance the SR-Algorithms robustness at low SNRs for contiguous sources. This mitigates noise sensitivity and inaccurate estimates with a fewer sensors at low SNRs by combining group-delay and SR techniques. The GDF is used to re-weight the inaccurate sparse estimate to obtain new results with very low estimation errors.

Considering Eq. (3), the SVD of the array data matrix can be re-written as:

$$\{\mathbf{y}(t)\}_{t=1}^{L} = \mathbf{U}\mathbf{\Lambda}\mathbf{V}^H = [\mathbf{U}_S \ \mathbf{U}_N]\mathbf{\Lambda}\mathbf{V}^H, \tag{9}$$

where $\mathbf{y}(t)$ is the received signal; $\mathbf{U}$ and $\mathbf{V}$ are the left and right singular matrices. The columns of $\mathbf{U}_S$ are the source singular vectors corresponding to the J largest singular values of $\mathbf{Y}$. On the other hand, the noise singular vectors are the columns of $\mathbf{U}_N$ corresponding to the $N - J$ smallest singular values of $\mathbf{Y}$. Now, the full overcomplete basis matrix $\mathbf{A}_\Omega$ can be decomposed as $\mathbf{A}_\Omega = [\mathbf{A} \quad \mathbf{B}]$ where $\mathbf{A} \in \mathbb{C}^{N\times J}$ correspond to the true source directions and $\mathbf{B} \in \mathbb{C}^{N\times K-J}$ to other directions. Let us define :

$$\mathbf{Z} = \mathbf{A}_\Omega^H\mathbf{U}_N = [\mathbf{A}^H\mathbf{U}_N \ \mathbf{B}^H\mathbf{U}_N] = [\mathbf{Q}_A \ \mathbf{Q}_B], \tag{10}$$

where $\mathbf{Q}_A \in \mathbb{C}^{J\times(N-J)}$ and $\mathbf{Q}_B \in \mathbb{C}^{(K-J)\times(N-J)}$ are some non-zero matrices. For the true data matrix, $\mathbf{Q}_A$ will be a zero matrix, but for the limited time sampled data matrix, $\mathbf{Q}_A$ will have values close to zero. Taking the phase response of the matrix, we get:

$$\begin{aligned}\angle\{\mathbf{A}_\Omega^H\mathbf{U}_N\} &= [\angle\{\mathbf{A}^H\mathbf{U}_N\} \ \angle\{\mathbf{B}^H\mathbf{U}_N\}] \\ &= [\angle\mathbf{Q}_A \ \angle\mathbf{Q}_B] = [\mathbf{\Phi}_A \ \mathbf{\Phi}_B],\end{aligned} \tag{11}$$

where $\angle(\cdot)$ calculates the wrapped phase spectrum of each column. It is worth noticing that the complex values of $\mathbf{Q}_A$ are small due the orthogonality property of signal and noise subspace. Thus, evaluating the phase response, i.e., $\mathbf{\Phi}_A \in \mathbb{C}^{J\times(N-J)}$ will result in sharp phase shifts as compared to $\mathbf{\Phi}_B \in \mathbb{C}^{(K-J)\times(N-J)}$.The phase spectrum changes differently near the true DOA locations. To capture the changes at the DOA, we calculate the group-delay by differentiating Eq. (11) with respect to θ. Numerically, we take the gradient of

each column of the Eq. (11) given as:

$$\nabla\angle\{\mathbf{A}_{\Omega}^{H}\mathbf{U}_N\} = [\nabla\angle\{\mathbf{A}^{H}\mathbf{U}_N\}\ \ \nabla\angle\{\mathbf{B}^{H}\mathbf{U}_N\}] = [\nabla\Phi_A\ \nabla\Phi_B] = [\boldsymbol{\tau}_A\ \boldsymbol{\tau}_B], \quad (12)$$

where $\nabla(\cdot)$ is equivalent to calculating the gradient of the unwrapped phase spectrum. Here, $\boldsymbol{\tau}_A \in \mathbb{C}^{J\times(N-J)}$ and $\boldsymbol{\tau}_B \in \mathbb{C}^{(K-J)\times(N-J)}$. As we are moving from non-DOA locations to DOA locations from any direction, there will be a shift in the values of the phase spectrum as explained in Eq. 11. While calculating the gradient, the sharp peaks at the DOA positions will be registered. Further, such peaks are less dependent on the number of sensors. Thus, we obtain the group-delay weight as given below:

$$(\mathbf{w}_{gd})^{-1} = [[\boldsymbol{\tau}_A^{(\ell_2)}]^T\ [\boldsymbol{\tau}_B^{(\ell_2)}]^T]^T. \quad (13)$$

where $\boldsymbol{\tau}_A^{(\ell_2)}$ is $[J\times 1]$ and $\boldsymbol{\tau}_B^{(\ell_2)}$ is $[(K-J)\times 1]$. It may be noted that $\boldsymbol{\tau}_A^{(\ell_2)}, \boldsymbol{\tau}_B^{(\ell_2)}$ are obtained by taking an incoherent sum over all the squares of columns of $\boldsymbol{\tau}_A$ and $\boldsymbol{\tau}_B$ matrices respectively, as computed by summing over the square of group delay values for all singular vectors.

Consider Eq.(10), those rows of $\mathbf{Z}$ which correspond to the source signal matrix $\mathbf{S}$ are small as compared to the entries in the other rows of $\mathbf{Z}$. Let $\mathbf{z}(j) = [z_1(j), \ldots, z_K(j)]^T$ be the j^{th} column of matrix $\mathbf{Z}$, for $j = 1, \ldots, N-J$. Let us define w_k by taking ℓ_2 norm of each row of $\mathbf{Z}$, i.e, $w_k = \sqrt{\sum_{j=1}^{N-J}|z_k(j)|^2}$, $k = 1, \ldots, K$, and combining $w_1, \ldots, w_k$, we obtain $\mathbf{w}_m = [w_1, \ldots, w_K]$. The $\mathbf{w}_m$ corresponds to the weights from the MUSIC magnitude spectrum.

To enhance the stability of the DOA estimates in case of heavy noise and array perturbations, we multiply the weights of group delay function with weight vector computed for the MUSIC magnitude spectrum. This results in MUSIC Group Delay (MGD) weights ($\mathbf{w}_{mgd}$), which are as follows:

$$\mathbf{w}_{mgd} = \mathbf{w}_{gd} \cdot \mathbf{w}_m. \quad (14)$$

Diagonalizing the weight vector of MGD ($\mathbf{w}_{mgd}$), we obtain the weight matrix as shown below:

$$\mathbf{W} = \text{diag}\,(\mathbf{w}_{mgd}) \quad (15)$$

Once the weights are obtained and after diagonalization as given in Eq. (15), the ℓ_1-SVD minimization in Eq. (8) is modified as:

$$\min||\mathbf{W}\bar{\mathbf{s}}^{(\ell_2)}||_1 \text{subject to} ||\tilde{\mathbf{Y}} - \mathbf{A}\tilde{\mathbf{S}}||_F^2 \leq \eta^2, \quad (16)$$

Thus, the position/location of largest peaks of $\mathbf{W}\bar{\mathbf{s}}^{(\ell_2)}$ provides an estimate of the source locations.

3.1. Re-weighting using linearly combined weights

For contiguous sources, the side-lobes for MGD-ℓ_1-SVD are not smooth near DOAs. The amplitude of such minor peaks could be dependent upon the noise levels and for the particular choice of regularization parameter η (for MGD-ℓ_1-SVD). Further, these minor peaks reduce the source separability. Thus, it becomes important not only to correctly resolve the closely spaced sources, but also to minimize the minor-peaks in the side lobe levels.

To achieve this, we combine the weights from different weighing regimes to obtain an optimal weights for the ℓ_1 minimization (Eq.(16)). Hence, the main objective of this proposed method ($\mathbf{w}_{opt}$-ℓ_1-SVD) is to obtain a highly resolved, robust, and smooth side-lobed DOA estimates. In this work, the optimal weights ($\mathbf{w}_{opt}$) are obtained by taking a linear combination of MUSIC weights (smooth side-lobes), $\mathbf{w}_m$ and the MGD weights, $\mathbf{w}_{mgd}$:

$$\mathbf{w}_{opt} = \alpha\,\mathbf{w}_{mgd} + \beta\,\mathbf{w}_m \quad (17)$$

where $\alpha, \beta \in [0, 1]$ and $\alpha + \beta = 1$. The value of α and β are selected such that the ARMSE [8] is minimized and resolution probability [6] is maximized simultaneously. The optimal value of α and β is found to be approximately 0.75 and 0.25, respectively, at -10 dB SNR. Similarly, for other values of SNR, the optimal value of α and β can be found.

4. Performance Evaluation

The performance of the proposed algorithms is analyzed on simulated data and compared with algorithms for various metrics. The measurements are taken from a Uniform Linear Array (ULA) with the inter-element spacing of half-wavelength. The simulation results are generated for contiguous sources at low SNR values. For multiple-snapshot processing, the number of snapshots taken is $L = 200$ [33]. The two sources are placed in between the broadside and the end-fire direction, i.e., $45^o, 52^o$, in order to gauge the efficiency of the proposed methodologies. These values are taken to check source separability of the algorithms at low SNR ranges [33] and with a fewer sensors. All the results are obtained over $10^2 - 10^3$ Monte-Carlo simulation and $N = 6$ for all algorithms unless stated explicitly.

4.1. ARMSE vs. SNR

In the first phase of the investigation, we evaluate the performance of the proposed algorithms through the ARMSE plots at different SNR values. Fig. 1 shows the ARMSE plot for various algorithms with 6 sensors at different SNR ranges in Gaussian Noise. The performance of MUSIC-ℓ_1-SVD and ℓ_1-SVD degrades significantly with few sensors. This might be because such algorithms cannot resolve both the sources correctly due to a lack of adequate measurements. This results in large ARMSE values for these methods. With less number of sensors and low SNR values, the MGD-ℓ_1-SVD and $\mathbf{w}_{opt}$-ℓ_1-SVD outperforms other algorithms in terms of ARMSE values for the noise.

4.2. Resolution Probability

The resolving capability of different algorithms in terms of probability of separability is shown in Fig. 2. It can be seen

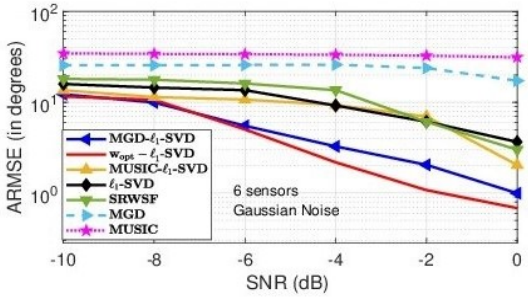

Figure 1: *ARMSE versus SNR plots for two spatially contiguous and uncorrelated sources.* $L = 200$

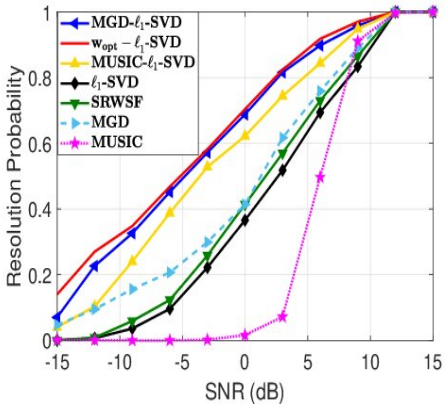

Figure 2: *Resolution probability versus SNR plot for spatially contiguous sources for different algorithms.*

from Fig. 2 that $\mathbf{w}_{opt}$-ℓ_1-SVD and MGD-ℓ_1-SVD has a better-resolving probability of closely spaced sources. At high SNR values ($>$ 10 dB), all different algorithms achieve almost similar estimation accuracy. The DOA estimation of closely placed sources at low SNRs results in large estimation errors. Even if the sources are resolved correctly, a small bias value is always present due to the sparsity prior (ℓ_1) in the objective function. A small bias would be considered as a good compromise.

4.3. Power Spectrum Analysis

In this section the power spectrum analysis with respect to the spatial angle (θ) is being done. Fig. 3 show the power spectrum for different algorithms with a closely spaced sources in Gaussian noise. With a fewer sensors, the MUSIC algorithm,ℓ_1-SVD, MUSIC-ℓ_1-SVD (SR algorithm re-weighted with MUSIC magnitude weights) [33, 17] and Sparse Recovery using Weighted Subspace Fitting (SRWSF) [6] fails to correctly resolve the sources in noise. It's evident that the enhanced resolution property of MGD-ℓ_1-SVD and $\mathbf{w}_{opt}$-ℓ_1-SVD results in better separation of sources than any other methods. The proposed methodologies are able to resolve both the closely and widely spaced sources significantly. It could also be noted that some bias error is present, which could be due to the use of the group-delay function. The minor peaks in side-lobes of MGD-ℓ_1-SVD appear to be reduced in the $\mathbf{w}_{opt}$-ℓ_1-SVD spectrum.

4.4. ARMSE vs. Number of Snapshots

The ARMSE versus number of snapshots performance is evaluated in Fig. 4 for incident signals at $(\theta) = 3.4°$. The signal and noise singular vectors subsequently asymptotically approaches the true signal and noise singular vectors, respectively. Further, the calculation of the weight vector/matrix in such methods is also based on the SVD of the array data matrix. Hence, the number of snapshots used for the estimated process plays a vital role in robust and unbiased estimation. It's evident from the figure that MUSIC and MGD have large ARMSE values for the set configuration. On the other hand, the SR based methods have low values of ARMSE for various range of snapshots. For closely placed sources in Gaussian noises, it is worth noticing that MGD-ℓ_1-SVD and $\mathbf{w}_{opt}$-ℓ_1-SVD has lower ARMSE values for a fewer numbers of snapshots. Thus, the MGD-ℓ_1-SVD and $\mathbf{w}_{opt}$-ℓ_1-SVD algorithms become a suitable choice for source localization & separation.

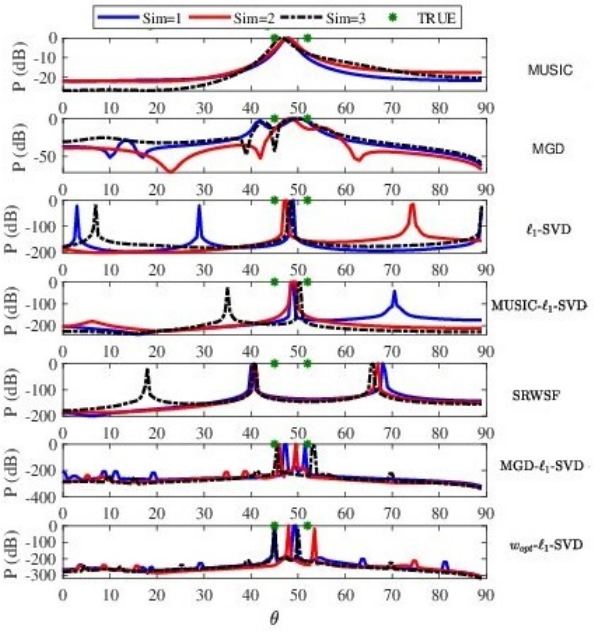

Figure 3: *Power spectrum for different algorithms with two sources separated by 7^o at -6 dB SNR with 6 sensors.*

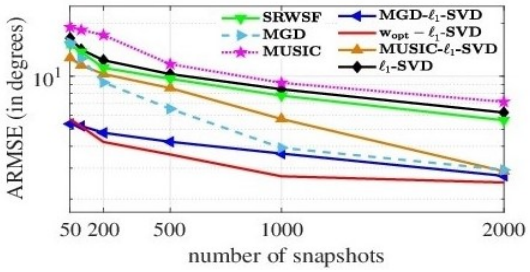

Figure 4: *ARMSE vs No. of snapshots for contiguous sources*

5. Conclusion

The proposed methodology has proven to bring more sparsity, robustness and enhance the resolution of source separability by SR algorithms under unfavorable conditions. With the use of adaptive grids, a few sensors, and a few sources ($J < L$), the computational complexity of the SR algorithm to resolve the sources is also reduced. The optimal weighting technique has enhanced the performance in terms of minimum ARMSE error and probability of separability particularly at low SNRs. The proposed re-weighted scheme has shown high performance with respect to the number of snapshots, resolution probability and even with contiguous sources.The proposed method would be instigated on different noises in the near future.

6. Acknowledgement

This work is supported by SERB Govt. of India, through Project No. CRG/2018/003920 under the CRG-SERB Scheme.

7. References

[1] H. L. V. Trees, *Optimum Array Processing: Part IV of Detection, Estimation, and Modulation Theory*. Melbourne, FL, USA: John Wiley & Sons, Inc., 2002.

[2] F. B. Jensen, W. A. Kuperman, M. B. Porter, and H. Schmidt, *Computational Ocean Acoustics (Modern Acoustics and Signal Processing)*. Springer, 2011.

[3] S. N. Bhuiya, F. Islam, and M. Matin, "Analysis of direction of arrival techniques using uniform linear array," *International Journal of Computer Theory and Engineering*, vol. 4, pp. 931–934, 01 2012.

[4] J. Capon, "High-resolution frequency-wavenumber spectrum analysis," *Proceedings of the IEEE*, vol. 57, no. 8, pp. 1408–1418, 1969.

[5] A. M. Elbir, "DeepMUSIC: Multiple signal classification via deep learning," *IEEE Sensors Letters*, pp. 1–1, 2020.

[6] N. Hu, Z. Ye, D. Xu, and S. Cao, "A sparse recovery algorithm for DOA estimation using weighted subspace fitting," *Signal processing*, vol. 92, no. 10, pp. 2566–2570, 2012.

[7] P. G. Angeliki Xenaki and K. Mosegaard, "Compressive beamforming," *Acoustical Society of America*, vol. 136, no. 1, pp. 260–271, Jul. 2014.

[8] D. Malioutov, M. Cetin, and A. S. Willsky, "A sparse signal reconstruction perspective for source localization with sensor arrays," *IEEE Trans. Signal Process.*, vol. 53, no. 8, pp. 3010–3022, 2005.

[9] C.F.Mecklenbräuker, P. Gerstoft, and A. Xenaki, "Multiple and single snapshot compressive beamforming," *Acoustic Society of America*, 2015.

[10] B. Lin, J. Liu, M. Xie, and J. Zhu, "Sparse signal recovery for direction-of-arrival estimation based on source signal subspace," *Journal of Applied Mathematics*, vol. 2014, 2014.

[11] Z.-M. Liu, Z.-T. Huang, and Y.-Y. Zhou, "Sparsity-inducing direction finding for narrowband and wideband signals based on array covariance vectors," *IEEE Transactions on Wireless Communications*, vol. 12, no. 8, pp. 3896–3907, 2013.

[12] H. Liu, L. Zhao, Y. Li, X. Jing, and T.-K. Truong, "A sparse-based approach for doa estimation and array calibration in uniform linear array," *IEEE sensors journal*, vol. 16, no. 15, pp. 6018–6027, 2016.

[13] C. Stoeckle, J. Munir, A. Mezghani, and J. A. Nossek, "DOA estimation performance and computational complexity of subspace- and compressed sensing-based methods," in *WSA 2015; 19th International ITG Workshop on Smart Antennas*. VDE, 2015, pp. 1–6.

[14] X. Hu, N. Tong, Y. Guo, and S. Ding, "Mimo radar 3-d imaging based on multi-dimensional sparse recovery and signal support prior information," *IEEE Sensors Journal*, vol. 18, no. 8, pp. 3152–3162, 2018.

[15] E. J. Candès and C. Fernandez-Granda, "Towards a mathematical theory of super-resolution," *Communications on pure and applied Mathematics*, vol. 67, no. 6, pp. 906–956, 2014.

[16] D. Wipf and S. Nagarajan, "Iterative reweighted ℓ_1 and ℓ_2 methods for finding sparse solutions," April 2004.

[17] F. Liu, L. Peng, M. Wei, P. Chen, and S. Guo, "An improved L_1-SVD algorithm based on noise subspace for DOA estimation," *Progress In Electromagnetics Research C*, vol. 29, pp. 109–122, 2012.

[18] Z. Yang and L. Xie, "Enhancing sparsity and resolution via reweighted atomic norm minimization," *IEEE Transactions on Signal Processing*, vol. 64, no. 4, pp. 995–1006, 2015.

[19] D. Needell, "Noisy signal recovery via iterative reweighted L1-minimization," in *Conference Record of the Forty-Third Asilomar Conference on Signals, Systems and Computers*. IEEE, 2009, pp. 113–117.

[20] H. A. Murthy and B. Yegnanarayana, "Formant extraction from group delay function," *speech communication*, vol. 10, no. 3, pp. 209–221, 1991.

[21] K. Nathwani, P. Pandit, and R. M. Hegde, "Group delay based methods for speaker segregation and its application in multimedia information retrieval," *IEEE transactions on multimedia*, vol. 15, no. 6, pp. 1326–1339, 2013.

[22] J. Sebastian and H. A. Murthy, "Group delay based music source separation using deep recurrent neural networks," in *2016 International Conference on Signal Processing and Communications (SPCOM)*. IEEE, 2016, pp. 1–5.

[23] K. Nathwani and R. M. Hegde, "Joint source separation and dereverberation using constrained spectral divergence optimization," *Signal processing*, vol. 106, pp. 266–281, 2015.

[24] K. Nathwani, A. Kumar, and R. M. Hegde, "Monaural speaker segregation using group delay spectral matrix factorization," in *2014 Twentieth National Conference on Communications (NCC)*. IEEE, 2014, pp. 1–6.

[25] J. Yadav, M. S. Fahad, and K. S. Rao, "Epoch detection from emotional speech signal using zero time windowing," *Speech Communication*, vol. 96, pp. 142–149, 2018.

[26] M. Shukla and R. M. Hegde, "Significance of the music-group delay spectrum in speech acquisition from distant microphones," in *International Conference on Acoustics, Speech and Signal Processing*. IEEE, 2010, pp. 2738–2741.

[27] L. Kumar, R. Mandala, and R. M. Hegde, "Music-group delay based methods for robust DOA estimation using shrinkage estimators," in *7th Sensor Array and Multichannel Signal Processing Workshop (SAM)*. IEEE, 2012, pp. 281–284.

[28] L. Kumar, A. Tripathy, and R. M. Hegde, "Robust multi-source localization over planar arrays using music-group delay spectrum," *IEEE Transactions on Signal Processing*, vol. 62, no. 17, pp. 4627–4636, 2014.

[29] L. Kumar, K. Singhal, and R. M. Hegde, "Robust source localization and tracking using music-group delay spectrum over spherical arrays," in *5th International Workshop on Computational Advances in Multi-Sensor Adaptive Processing*. IEEE, 2013, pp. 304–307.

[30] C. F. Mecklenbräuker, P. Gerstoft, E. Zöchmann, and H. Groll, "Robust estimation of doa from array data at low snr," *Signal Processing*, vol. 166, p. 107262, 2020.

[31] R. G. Baraniuk, "Compressive sensing," *IEEE Signal Processing Magazine*, vol. 118, Jul. 2007.

[32] D. L. Donoho, M. Elad, and V. N. Temlyakov, "Stable recovery of sparse overcomplete representations in the presence of noise," *IEEE Transactions on information theory*, vol. 52, no. 1, pp. 6–18, 2005.

[33] A. Koul, G.V.Anand, S. Gurugopinath, and K. Nathwani, "Three-dimensional underwater acoustic source localization by sparse signal reconstruction techniques," *In International Conference on Signal Processing and Communications*, 2020.